A STEREO PHOTOGRAPHY SYSTEM FOR MONITORING FULL FIELD THICKNESS VARIATION DURING RESIN INFUSION

Q. Govignon [1], S. Bickerton [1], J. Morris [2], and J. Lin [2]

[1]Centre for Advanced Composite Materials, Department of Mechanical Engineering
[2]Communication & Information Technology Research, Dept. of Computer Science
The University of Auckland, Private Bag 92019, AUCKLAND, NEW ZEALAND
Corresponding Author's e-mail: s.bickerton@auckland.ac.nz

ABSTRACT: This paper focuses on laminate thickness measurement during the Resin Infusion process. It is part of a larger project to establish a comprehensive data acquisition system for characterisation of this complex process. The acquisition of detailed thickness data is motivated by the need to develop an accurate simulation tool for Resin Infusion. After presenting several compaction studies on a typical glass fibre fabric, the paper will quickly review the current techniques used to monitor laminate thickness evolution, highlighting the disadvantages of single point measurement methods. Stereophotography offers the possibility of full field measurement of laminate thickness, a brief introduction to the theory being presented here. Initial results show the potential of the technique, though an improvement is required in the image reconstruction algorithm to obtain the thickness resolution required.

KEYWORDS: VARI, Thickness measurement, Stereophotography, Compaction.

INTRODUCTION

The Resin Infusion process (a.k.a. VARI, VARTM, SCRIMP, RIFT) has developed as a low cost method for manufacturing large composite parts. It has been used mainly to produce structural parts for the marine, civil, and military sectors [1, 2]. It has also been shown that aircraft quality composite structures can be produced [3, 4]. However, the process still presents some challenges to industry with regards reliability and repeatability. Due to the complex nature of the Resin Infusion process, trial and error development is expensive and inefficient. Therefore a comprehensive simulation model of the VARTM process is required.

Resin Infusion is a closed mould Liquid Composite Moulding (LCM) process that presents some similarities to Resin Transfer Moulding (RTM). The current analysis schemes adopted for RTM flow simulations assume resin flow through the preform behaves as flow through a porous medium. The modelling of porous flow is governed by Darcy's law:

$$\langle v \rangle = -\frac{1}{\mu}[K]\nabla P \tag{1}$$

where $\langle v \rangle$ is the fluid averaged velocity vector, μ is the fluid viscosity, K the permeability tensor for the preform, and ∇P is the local pressure gradient in the resin.
For Resin Infusion, two-part rigid moulds are replaced by single side rigid moulds sealed with a vacuum bag. Bag flexibility induces a new aspect absent in RTM: the thickness of the laminate being dependent on local resin pressure. During processing both the transfer of the

matrix and the compaction of the reinforcement are achieved using one atmosphere of pressure. Compaction stress supported by the reinforcement is therefore a balance between atmospheric pressure and the resin pressure:

$$\sigma_f = P_{ATM} - P \qquad (2)$$

Due to the variation of resin pressure in the laminate during mould filling and post-filling, laminate thickness varies during both the mould filling and post filling stages. It is therefore important to be able to accurately monitor these thickness changes, which may significantly affect reinforcement permeability and thus resin flow.

Previous studies by the authors have employed laser gauges to provide point measurements of laminate thickness [5]. Inconsistent results have prompted the development of a system capable of simultaneously capturing the thickness field of an entire laminate. Previous work by Anderson et al. concerned the development of a stereophotographic system to measure thickness using specialised CCD cameras [6]. This paper introduces the development of a stereophotographic system using general use cameras and alternative algorithms to reduce setup costs. Efforts will also be made to improve thickness resolution and increase the field of measurement.

REINFORCEMENT COMPACTION

Consider evolution of reinforcement fibre volume fraction (V_f) during different phases of a typical Resin Infusion process. Vacuum is applied initially to the reinforcement before resin injection. The reinforcement supports all of the externally applied pressure ($\sigma_f = P_{ATM}$) and a dry maximum V_f is reached. During resin infiltration, two deformation mechanisms occur in the wetted portion of the laminate. As the flow front passes a particular point a local increase in V_f occurs, due to the lubricating effect of the fluid causing a rearrangement of fibres in the reinforcement. The resin pressure locally is low ($P \approx 0$) and the compaction pressure high ($\sigma_f \approx P_{ATM}$), thus V_f increases. As the flow front progresses past this point resin pressure increases, the compaction stress applied to the reinforcement decreases, and a decreases in V_f occurs. Finally, once the mould is filled and resin flow to the inlet is stopped, resin pressure throughout the laminate slowly decreases, and a higher V_f is recovered.

The compaction response of a laminate depends on a number of material parameters including fibre material, reinforcement architecture, and number of fabric layers. Process parameters such as compaction speed also play a role. Compaction speed, number of layers, and resin presence are explored experimentally below.

Experimental Setup

The reinforcement used in this study is an 821g/m² biaxial stitched glass fabric (balanced 0-90°). Circular samples were cut to a diameter of 200 mm. The compaction experiments were performed using a two piece aluminium mould mounted in an Instron 1186 testing machine. The Instron was used in load control mode, allowing specific compaction stresses to be applied to the samples. The major advantage of the testing machine is high accuracy in the measurement of the displacement and load. However, care must be taken in the setup of the mould, as small errors in cavity thickness lead to significant V_f discrepancies. Significant care was taken to ensure that the mould platens were well aligned, and that zero cavity thickness was well established.

Influence of Loading Rate

The first set of compaction experiments were performed to determine the influence of the applied load rate. For simplicity, a test fluid was not introduced to simulate the presence of resin. Samples composed of 6 fabric layers were progressively loaded to a compaction stress of 1.0 bar at a constant loading rate. Load was held constant at this level for 5 minutes allowing creep to take place. The load was then removed at the same rate until an equivalent stress of 0.2 bar was achieved, and another period of constant force was applied. A set of five tests were performed at each of the load rates 0.2, 0.4 and 0.6 kN/min. These speeds were chosen as they roughly approximate the loading rates applied during initial application of vacuum to a dry laminate.

Table 1: Influence of the loading rate on the resulting V_f.

Compaction speed	0.2kN/min	0.4kN/min	0.6kN/min
Mean maximum V_f	53,20%	52,99%	52,83%
Mean V_f after unloading	51,67%	50,56%	50,04%

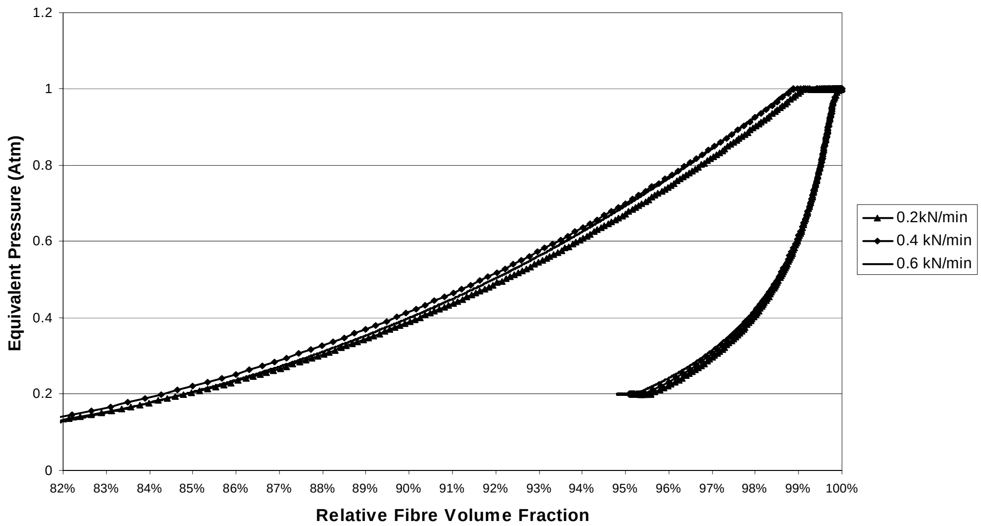

Figure 1: Comparison of the compaction behaviour at various loading rate.

The fibre volume fractions achieved after initial application of vacuum and after unloading to 0.2 bar are presented in Table 1 (averaged across five tests). V_f is seen to decrease slightly with increasing loading rate, the samples showed increasing rigidity. Figure 1 presents V_f versus compaction stress traces for three typical experiments. These traces have been normalised against the maximum V_f achieved, to highlight any significant differences between the shapes of the curves. Considering the similarities between these curves, and the V_f data presented in Table 1, loading rate is assumed to have negligible effect for the remainder of this study. Therefore, the remainder of the tests were performed at a loading rate of 0.6 kN/min.

Influence of the Number of Layers

It has been widely documented that the number of layers of reinforcing fabric significantly influences the compaction behaviour of a laminate [7, 8]. The strength of this effect depends on the architecture of the reinforcement. To study the strength of this effect for the biaxial fabric, compaction samples composed of 3, 6, 9, 12 and 15 layers have been tested. The same compaction strategy was applied as above. Table 2 presents the V_f values achieved at various stages, in each case being an average of five tests. The V_f values diminish with increasing numbers of layers, but do not approach a limit. Figure 2 presents V_f versus compaction stress traces for five typical experiments, with the data being normalised against the maximum V_f. This figure demonstrates a high degree of similarity between four of the curves, the overall behaviour being very similar for samples composed of at least 6 layers. Samples of 6 layers were used for the remaining compaction studies.

Table 2: Influence of the number of layers on the V_f.

Number of layers	3	6	9	12	15
Mean V_f after first compaction	52,5%	50,2%	49.7%	49.4%	49,3%
Mean V_f after unloading	50,2%	48,0%	47.6%	47.3%	47,1%
V_f after second compaction	52,9%	50,8%	50.3%	50.1%	49,9%

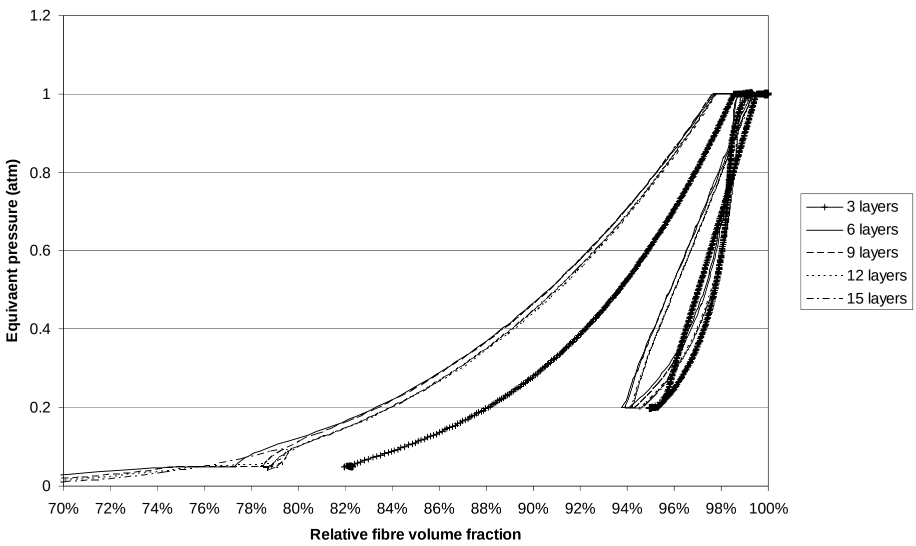

Figure 2: Compaction curves related to the maximum volume fraction for different number of layer.

Wet Compaction Response

Compaction experiments were completed to demonstrate the influence of the presence of a viscous fluid. Another focus of this study was the application of different pressures at vents during filling and post-filling, following on from previous studies exploring the possibility for V_f control [5]. Samples of 6 layers were subject to a similar compaction strategy as described above, using a loading rate of 0.6 kN/min. For these experiments, fluid was injected slowly into the reinforcement following the initial period of holding at 1.0 bar. This pressure was maintained constant, allowing any further relaxation to occur due to the presence of the fluid. The reminder of the test was carried out as described above. This compaction cycle was modified to simulate the use of different pressures during processing. Pressure at the vents during filling and post-filling were set at values of 0.01, 0.3, and 0.5 bar. The various strategies applied are detailed in Table 3.

Table 3 presents V_f's achieved at three instances in the compaction cycle. The final column in this table presents the V_f achieved at completion of the process, essentially the V_f of the finished product. This data presents a small potential for controlling the V_f of the resulting composite (48.2 to 51.8%), which appears to depend only on the pressure applied during post-filling. These results do not reflect the larger degree of V_f control demonstrated in a previous study of the actual resin infusion process [5], in which a V_f range between 47.1 and 59.1% were achieved for the same biaxial fabric. In that study it was shown that pressure levels set during both filling and post-filling significantly influenced the final V_f of the laminate. Method A (according to Table 3) gave the largest V_f of 59.1%, and method E the lowest value of 47.1%. It should be noted that V_f data for this Resin Infusion study was determined by measuring mass fraction of the resulting laminates. This method does not account for any residual void content. However, visual inspection of the laminates leads the authors to believe that void content is not the sole reason for discrepancies between the compaction studies described here, and the previous Resin Infusion tests. Such discrepancies can be best explored by full field cavity thickness measurements. This issue has provided motivation for the stereophotography equipment described below.

Table 3: Result of the wet compaction tests.

Vacuum pressure during mould filling / postfilling (mbar)	Method	V_f after first compaction	V_f after unloading	V_f after second compaction
500/10	A	47,68%	46,60%	51,50%
300/10	B	49,10%	47,42%	51,66%
10/10	C	50,54%	48,05%	51,82%
500/300	D	47,29%	46,27%	49,32%
300/500	E	48,83%	47,16%	48,83%
300/300	F	48,70%	47,17%	49,65%
500/500	G	47,66%	45,95%	48,20%
10/300	H	50,93%	48,44%	50,83%
10/500	M	51,14%	48,61%	50,11%

THICKNESS VARIATION MEASUREMENT DURING RESIN INFUSION

Laser Gauges

Variations of laminate thickness during Resin Infusion are very influential, mould filling times being affected by the variations in V_f, and hence reinforcement permeability. Thickness variations have been measured in the past using LVDTs. These sensors rely on contact, and for that reason apply a limited but measurable stress to the laminate [9]. Laser gauges have also been used as a non-contact option [5], but along with LVDTs, they provide measurements only at a single point. Another drawback of laser gauges is the very small sampling area; the thickness data may have significant variation depending on the place of the measurement, whether made at the centre of a fibre tow, or between two tows. Figure 3 presents sample laminate thickness data from four Resin Infusion tests, performed without distribution media. In each case 12 layers of the biaxial fabric were employed, being infused with mineral oil, under identical conditions. In all four tests an initial drop in laminate thickness is observed as the resin front passes the measurement position. Beyond this time the four traces exhibit quite different, and puzzling behaviour. Our ability to interpret this data is severely limited as measurement is completed at a single point, providing further motivation for development of full field measurements.

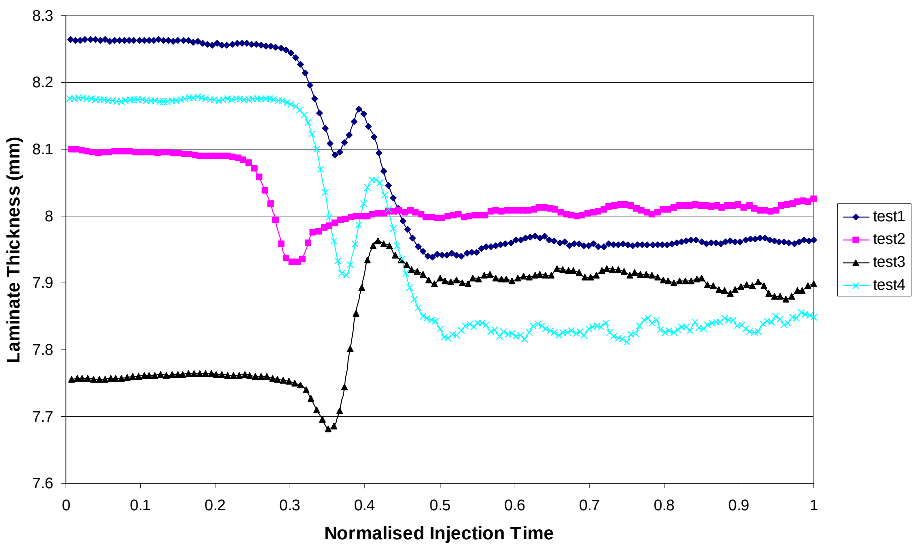

Figure 3: Comparison of the laser transducer reading on four similar experiments.

Stereophotography

Theory

Direct distance measurement techniques, *e.g.* laser range-finders and SONAR, scan a single probe beam through a scene and measure time-of-flight or phase differences from which distances are trivially derived. These techniques are relatively slow, being dependent on mechanical scanning systems, and thus not well suited to the acquisition of dense 3D maps of fast processes.

Stereophotography is based on triangulation - two cameras at different positions establish two lines to each binocularly visible point in the scene. This results in dense 3D environment maps at speeds determined by the rate at which images can be transferred from the cameras to a computer and processed. Figure 4 shows the arrangement used in our system. Note that we use a *verging* axis system to obtain better accuracy from our cameras - by maximising the number of binocularly visible points and using most of the image planes of each camera[10].

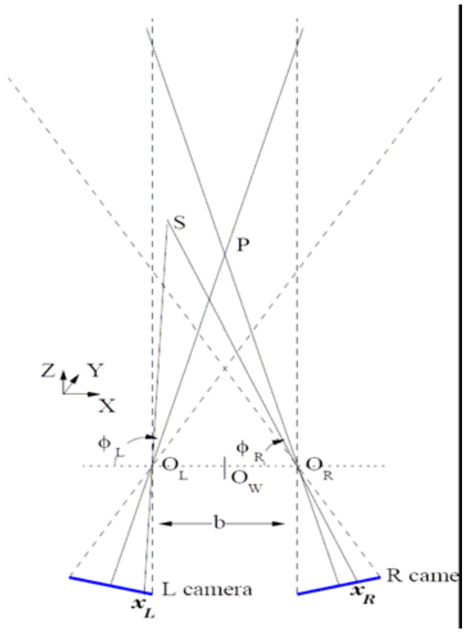

Figure 4: Stereo camera arrangement:
$O_{L|R}$ - optical centres of left—right cameras;
P - fixation point (intersection of camera optical axes);
S(X,Y) - scene point;
$x_{L|R}$ -x-coordinate of projection of S onto camera image planes;
$\phi_{L|R}$ - angles between optical axes and baseline;
b - camera separation

In Figure 4, two cameras are positioned with their optical centres separated by a distance, b, along the baseline and aligned at angles, ϕ_L and ϕ_R to the baseline. The optical axes intersect at the *fixation point*, *P*. A typical scene point, $S(X,Y,Z)$, appears at x_L in the left camera image and x_R in the right camera image. The difference, $d = x_L - x_R$ is known as the disparity. If world coordinates are referenced to an origin, O_W (mid-point of the baseline joining the camera optical centres) and axes X, Y and Z, as shown in Figure 4, then the coordinates of a scene point are:

$$X = \frac{b}{2}\frac{(f\tan\phi_R + x_R)(f - \tan\phi_L x_L) + (f\tan\phi_L + x_L)(f - \tan\phi_R x_R)}{(f\tan\phi_R + x_R)(f - \tan\phi_L x_L) - (f\tan\phi_L + x_L)(f - \tan\phi_R x_R)} \tag{3}$$

$$Z = -(\frac{b}{2} + X)\frac{f\tan\phi_L + x_L}{f - \tan\phi_L x_L} \tag{4}$$

(5)

$$Y = \frac{Z}{f\sin\phi_L} y_L \tag{5}$$

where *f* is the focal length. Thus, given a correct match between the points on the image planes (*xL, yL)* and (*xR, yR)* corresponding to a scene point (*X, Y, Z)*, the coordinates of the scene point can be discovered. In practice, determining a correct match automatically is a non-trivial problem. Fortunately, in this particular application, one major source of matching difficulties – occlusions or points visible in one camera only - will be absent: the smooth, continuous single surface of the mould enables smoothness and continuity constraints to be added to the matching algorithm. We have painted the surface of the mould with a fine, random pattern of coloured spots to provide sufficient texture to reduce the probability of false matches due to sensor noise, variations in reflectance with angle, *etc*. Furthermore, a small window of pixels (typically 9*9) was used as the basis for matching to reduce the effects of noise (We use the term 'noise' here to include all sources of intensity mismatch[10]).

Setup

Two Canon EOS 20D digital SLR Camera with resolution of 8.2 Mega-pixels are used for image acquisition. These cameras are mounted on a series of precision rotation stages, and a goniometer to allow for very precise alignment. The cameras are connected to two synchronized computers that control the cameras and store the images. The cameras must be aligned to converge exactly on the same point, ensuring they capture same plan area. Calibration is carried out using a precise grid, allowing for any inherent distortion of the camera lenses, and allowing the determination of the orientation and baseline between the cameras. Determination of the orientation and baseline are necessary for the triangulation process used to determine 3D shape of the subject.

To facilitate stereo-matching of the two images during the Resin Infusion processing, a random pattern is painted on the vacuum bag. This pattern must present very fine random features at a high frequency as the matching window is a square of 13*13 pixels. After several trials, the selected pattern is painted with spray-cans of cyan, magenta, and yellow, applying a random arrangement of very small paint droplets. It is also very important to provide good lightning to the subject, and to prevent any reflections on the surface. Reflections are usually affect each camera differently, causing major problems during image matching.

The stereophotography rig is mounted over a temperature controlled Resin Infusion table. Fluid pressures inside the laminate are measured at three locations using pressure transducers mounted on the underside of the table. Fluid flow rate into the laminate is monitored by continuously weighing the resin pot using a mass balance attached to the data acquisition computer.

Figure 5: Details of the stereophotography rig.

Results

Several reconstructed 3D images are presented in Figure 6. A snail model has been used previously to prove the technique, however, the depth variations in this object are much greater than those expected in a laminate during Resin Infusion. This model is 22 cm long and 12 cm wide, and includes small variations in texture having depth of 0.5 mm. A 3D reconstruction from a Resin Infusion experiment is also presented in Figure 6. The laminate was constructed of 10 layers of a 450 g/m² Continuous Filament Mat (CFM) fabric, 50 cm long and 27 cm wide. CFM was chosen for it's large thickness, and large thickness changes during processing. The 3D reproduction of the laminate thickness is covered with the actual texture captured by the cameras, providing a visually pleasing result. However, while the image appears to show a reasonable thickness variation behind the flow front, it has become clear during processing of the data that the current stereo-matching algorithm is incapable of resolving laminate thickness to the required accuracy. A resolution on the order of 0.03 mm is the goal of this work, but currently we are only able to achieve approximately 0.5 mm. Alternative matching algorithms have been sourced, and will be implemented in the near future.

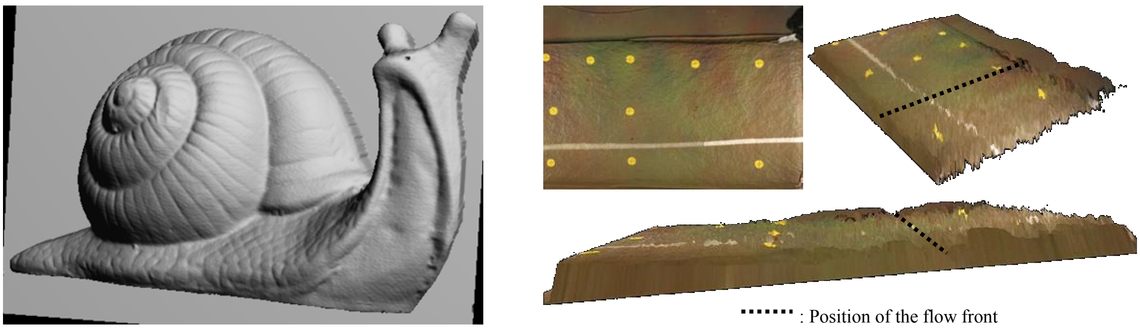

Figure 6: 3D images reconstructed using the Stereophotography technique.

CONCLUSION

The main focus of this study was to demonstrate the potential of full field laminate thickness measurement during the Resin Infusion process. Several compaction studies have been presented demonstrating the complex nature of fibre reinforcements, and the influence of several process parameters. The complexity of reinforcement compaction response motivates the detailed measurement of laminate thickness evolution, vital if accurate process simulations are to be developed. The disadvantages of single point measurement techniques has motivated the authors to develop a stereophotographic system for monitoring full field thickness variation. A full field measurement will help to explain spatial variations in laminate thickness, which appear to produce erratic results from experiment to experiment using single point techniques. An experimental facility has been established, and the technique validated against test 3D shapes. An initial Resin Infusion experiment has been subjected to the stereo technique, and while the results are visually pleasing, it is clear that the current image matching algorithm does not provide the accuracy of thickness resolution required. Efforts now focus on the implementation of an appropriate matching algorithm.

ACKNOWLEDGEMENTS

The authors thankfully acknowledge the funds received from the Foundation for Research, Science and Technology New Zealand to carry out this research. They also would like to acknowledge High Modulus (NZ) Ltd. for the donation of reinforcements.

REFERENCES

[1] G. Marsh, "Putting SCRIMP in context," *Reinforced Plastics*, vol. 41, pp. 22-26, 1997.

[2] C. Williams, J. Summerscales, and S. Grove, "Resin Infusion under Flexible Tooling (RIFT): a review," *Composites Part A: Applied Science and Manufacturing*, vol. 27, pp. 517-524, 1996.

[3] B. Berenberg, "Liquid composite molding achieves aerospace quality," *High-Performance Composites*, vol. 11, pp. 18-22, 2003.

[4] R. W. Koon, S. C. Parsons, L. K. Flansburg, and R. Loeslien, "VARTM of integrated secondary aircraft structure," presented at 34th International SAMPE Technical Conference, Baltimore, MD; USA, 2002.

[5] B. Daval and S. Bickerton, "Exploring the potential for laminate quality control using VARTM," in *36th Int. SAMPE Technical Conference*. San Diego, CA: SAMPE, 2004.

[6] H. M. Andersson, T. S. Lundstrom, B. R. Gebart, and P. Synnergren, "Application of Digital Speckle Photography to Measure Thickness Variations in the Vacuum Infusion Process," *Polymer Composites*, vol. 24, pp. 448-455, 2003.

[7] F. Robitaille and R. Gauvin, "Compaction of textile reinforcements for composites manufacturing. I: Review of experimental results," in *Polymer Composites*, vol. 19, 1998, pp. 198-216.

[8] P.A. Kelly, R. Umer, and S. Bickerton, "Viscoelastic response of dry and wet fibrous materials during infusion processes," *Composites Part A: Applied Science and Manufacturing*, vol. In Press, Corrected Proof.

[9] L. Joubaud, V. Achim, and F. Trochu, "Numerical simulation of resin infusion and reinforcement consolidation under flexible cover," *Polymer Composites*, vol. 26, pp. 417-427, 2005.

[10] J. Liu, P.J. Delmas, G. Gimel'farb, and J. Morris, "Stereo reconstruction using an image noise model," presented at Digital Image Computing: Techniques and Application (DICTA2005), Cairns, Australia, 2005.